



HAL
open science

High-pressure structure and electronic properties of YbD 2 to 34 GPa

S. Klotz, M. Casula, K. Komatsu, S. Machida, T. Hattori

► **To cite this version:**

S. Klotz, M. Casula, K. Komatsu, S. Machida, T. Hattori. High-pressure structure and electronic properties of YbD 2 to 34 GPa. *Physical Review B: Condensed Matter and Materials Physics* (1998-2015), 2019, 100 (2), 10.1103/PhysRevB.100.020101 . hal-02289321

HAL Id: hal-02289321

<https://hal.sorbonne-universite.fr/hal-02289321v1>

Submitted on 16 Sep 2019

HAL is a multi-disciplinary open access archive for the deposit and dissemination of scientific research documents, whether they are published or not. The documents may come from teaching and research institutions in France or abroad, or from public or private research centers.

L'archive ouverte pluridisciplinaire **HAL**, est destinée au dépôt et à la diffusion de documents scientifiques de niveau recherche, publiés ou non, émanant des établissements d'enseignement et de recherche français ou étrangers, des laboratoires publics ou privés.

High-pressure structure and electronic properties of YbD₂ to 34 GPaS. Klotz,^{1,*} M. Casula,¹ K. Komatsu,² S. Machida,³ and T. Hattori⁴¹*IMPMC, CNRS UMR 7590, Sorbonne Université, 4 Place Jussieu, F-75252 Paris, France*²*Geochemical Research Center, Graduate School of Science,**The University of Tokyo, 7-3-1 Hongo, Bunkyo-ku, Tokyo 113-0033, Japan*³*CROSS, Neutron Science and Technology Center, 162-1 Shirakata, Tokai, Ibaraki 319-1106, Japan*⁴*J-PARC Center, Japan Atomic Energy Agency, 2-4 Shirakata, Tokai, Ibaraki 319-1195, Japan*

(Dated: September 11, 2019)

Ytterbium dihydride (YbH₂) shows a well-known transition at ≈ 16 GPa from a CaH₂-type structure to a high-pressure (high-P) phase with Yb at hcp sites and unknown H-positions. Here, we report its complete structure determination by neutron diffraction at 34 GPa. Hydrogen (deuterium) is located at 2a and 2d positions of space group $P6_3/mmc$, thus forming a high-symmetry “collapsed” close-packed lattice. The transition is sluggish and can be seen as a transfer of 1/2 of the hydrogen atoms from strongly corrugated H-layers to interstitial sites of the Yb-lattice. We demonstrate by first-principles calculations that the transition is related to a change from a completely filled f -electron configuration to a fractional f -hole (≈ 0.25 h) occupation in the high-P phase. The $f \rightarrow d$ charge transfer closes the gap at the transition and leads to a metallic ground state with sizeable electron-phonon interaction involving out-of-plane vibrational modes of interstitial hydrogen.

There is considerable recent interest in hydrides under high pressure following the discovery of high- T_c superconductivity in H₂S compressed to 150 GPa [1]. Indeed, theory [2] and recent experiments [3] gives strong indications that superconductivity at elevated temperatures might occur in numerous hydrides, in particular binary rare-earth hydrides [4] with high hydrogen (H) content, which are unstable at ambient pressure. The case of Ytterbium (Yb) hydrides has so far not been investigated but appears to be interesting for the following reasons: Elemental Yb was recently found to be superconducting beyond 80 GPa [5]. This is highly unexpected, since Yb is diamagnetic at ambient conditions [6], and pressure is believed to turn it magnetic through a $f^{14} \rightarrow f^{13}$ (Yb²⁺ \rightarrow Yb³⁺) valence change [7] supported by EXAFS [8], XANES [5] and RIXS [9] data, thus unlikely to be superconducting.

This surprising finding draws attention to its most common hydride, YbH₂. This material is insulating and crystallizes at 0 GPa in the α -phase, whose structure is of CaH₂ orthorhombic type (space group $Pnma$) [10]. Under pressure, it transforms at ≈ 16 -20 GPa into a phase with Yb sites at a hexagonal close-packed (hcp) lattice [11]. The H atom positions are presently unknown. Again, this first-order transition ($\Delta V/V=3\%$) might be driven by a valence change of Yb from 2+ to 3+, as indicated by EXAFS [12]. The YbH₂ high-pressure (high-P) phase is stable to at least 60 GPa [12], its electronic properties are unknown.

Given this context, it appears timely to determine the full structure of YbH₂, i.e. the H position as well as its electronic properties beyond 16 GPa. Generally speaking, experimental data on the H location in high-P metal hydride phases are extremely sparse. Almost all structural information above a few GPa has been obtained

by synchrotron x-ray diffraction which is blind to H in the presence of heavy atoms. So far, the H positions are simply assumed to be on “favorable” interstitial sites, or deduced from first-principles calculations [13–15].

Here, we present high-P neutron diffraction data to 34 GPa which completely and unambiguously determine the structure of YbH₂, in particular the H positions. We use the structural data to determine its electronic properties through *ab initio* methods, which indicate a semiconducting-to-metal transition concomitant with the structural transformation. The metalization is driven by an $f \rightarrow d$ charge transfer with partial f -hole unbinding.

We used deuterated samples (YbD₂) for the well-known fact that H is a strong incoherent scatterer. From the x-ray diffraction data it is clear that deuteration has no significant structural effect, even at high pressure [12]. Ytterbium has 70 electrons and hence scatters ≈ 5000 times stronger than deuterium (D), i.e. an x-ray diffraction pattern is completely dominated by Yb. This is not the case for neutrons: the coherent neutron cross sections of Yb and D are 19.4 barn and 5.6 barn, i.e. are of the same order of magnitude. Neutron diffraction is most likely the only technique to solve the problem.

The sample was synthesized by heating Yb powder (99.9 % metal purity, fresh filings with ca 0.1 mm grain size from a rod purchased from Goodfellow) in 2000 hPa deuterium atmosphere to 600 °C, hence similar to the procedure described in previous work [10]. Neutron diffraction data of ground powder taken at ambient conditions in a vanadium can revealed single-phase material with the expected CaH₂ structure, space group $Pnma$, $a=5.8823(2)$ Å, $b=3.5676(1)$ Å, $c=6.7588(2)$ Å, and fractional atomic positions $x(\text{Yb})=0.2396(3)$, $z(\text{Yb})=0.1119(1)$, $x(\text{D1})=0.3556(3)$, $z(\text{D1})=0.4291(3)$, $x(\text{D2})=-0.0305(5)$, $z(\text{D2})=0.6784(3)$. As expected, the

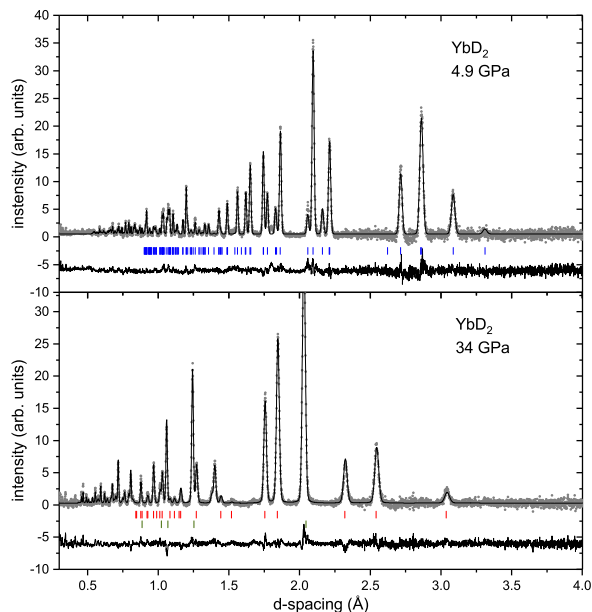


FIG. 1. Neutron diffraction patterns of YbD_2 at 298 K, in the low-P $Pnma$ phase (upper panel) and the high-P $P6_3/mmc$ phase (lower panel). The lines are Rietveld fits to the data (dots). Upper tickmarks indicate Bragg reflections of the sample, lower tickmarks of diamond from the anvils. $\chi^2=2.05$, $R_{wp}=7.95\%$ (top); $\chi^2=2.27$, $R_{wp}=8.05\%$ (bottom). Accumulation time is 1 hour and 2 hours, for 4.9 GPa and 34 GPa pressure, respectively.

compound is slightly non-stoichiometric with a refined D composition of 1.912(4) instead of 2. This is a well-known phenomenon and was observed in all previous studies on YbD_2 [10]. For the sake of simplicity, we will call the sample YbD_2 throughout the text.

Neutron diffraction measurements were carried out at the high-P beamline PLANET [16] at MLF, the Japan Proton Accelerator Research Complex (J-PARC), Tokai, Ibaraki, Japan. The three high-P runs used three types of double-toroidal sintered diamond anvils [17, 18] with maximum sample volumes of 12 mm^3 , 7 mm^3 and 3 mm^3 , encapsulating TiZr gaskets and a 4:1 methanol-ethanol mixture as pressure transmitting fluid. All runs applied a VX4-type Paris-Edinburgh load frame [17] with the position of the sample maintained to within $\pm 0.1 \text{ mm}$ relative to the laboratory frame. The pressure values cited here were determined from the equation of state (EOS) of YbD_2 reported by the x-ray work [12], using the measured ambient pressure unit cell volume ($V_0=141.84 \text{ \AA}^3$) for the low pressure (low-P) phase. In the first run to 22.6 GPa the sample was temporarily heated to 363 K in each pressure ramp-up to keep the sample hydrostatic up to 16 GPa. In the runs to 26 GPa and 34 GPa compressions were made at 299 K.

Fig. 1 shows diffraction patterns along with Rietveld refinements [19] of YbD_2 in the low-P α -phase at 4.9 GPa and in the high-P phase at 34 GPa. The transi-

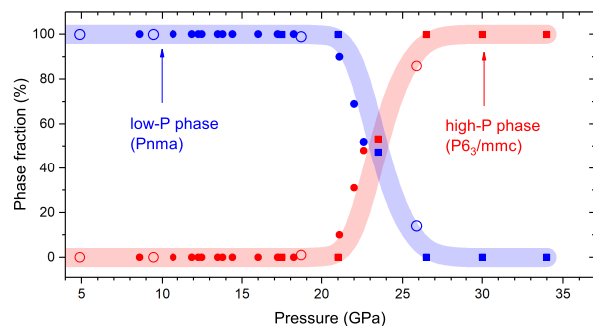


FIG. 2. Phase fraction of YbD_2 as pressure is increased (up-stroke). Filled circles, open circles and squares indicate three different runs to 22.6 GPa, 26 GPa and 34 GPa, respectively. Broad lines are guides to the eye.

tion is found to be sluggish in all runs, see Fig. 2, and heating to 363 K in the first loading had no significant effect on its kinetics. It starts at 20 GPa (approximately consistent with previous data) and ends slightly above 26 GPa, thus higher than what has been reported from x-rays studies [11].

The determination of the high-P structure is facilitated by the fact that the heavy-element (Yb) sublattice is known to be hcp [11] and the number of possibilities of incorporating H(D) therein with the required stoichiometry is limited. With Yb placed at the 2c position of space group $P6_3/mmc$, nine configurations were tested with H(D) on the remaining 2a, 2b, 2d and 4f positions. These include hence the tetrahedral (2a) and octahedral (4f) sites which are preferentially occupied by H(D) in various other hcp metals. Wyckoff sites with multiplicity 6, 12, and 24 would place H(D) on very low-symmetry sites with partial occupancy which hardly can be justified given the high-symmetry environment of the Yb-sublattice. Pattern simulations [20] show that out of these nine configurations, *only one* is compatible with the measured diffraction data, all others give strongly different intensities and hence can be safely excluded. The structure consists of one H(D) on the 2a position (on the octahedral hcp site) and the other on the 2d site, see Fig. 3. The refinement of the pattern at 34 GPa gives $a=3.5088(2) \text{ \AA}$, $c=4.6413(3) \text{ \AA}$. Apart from lattice constants, the refinements include only a minimal set of parameters, i.e. phase fraction, profile and preferred orientation. Interestingly, this H(D) configuration was guessed 36 years ago [10] from purely geometrical arguments applied to the low-P α -phase.

Inspection of the α -phase along its b -axis reveals an interesting relationship with the high-P phase, and details of the transition mechanism: In the α -phase, Yb is on a distorted hcp lattice, the c/b ratio at 15 GPa is 1.90 compared to 1.633 for an ideal hcp structure, and there are further small displacements along the orthorhombic a -axis. H(D) in this structure is stored in strongly corru-

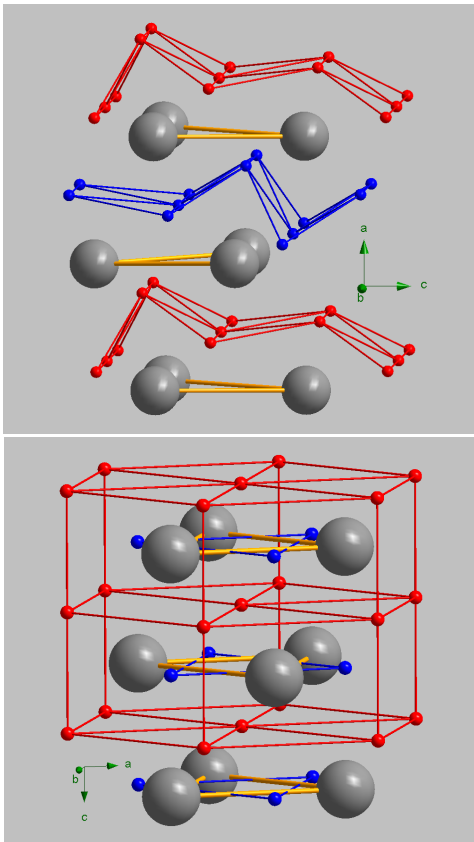


FIG. 3. Structure of YbD_2 in its low-P $Pnma$ (top) and the high-P $P6_3/mmc$ phases (bottom). Large symbols are Yb atoms, small symbols H(D). Different colors for H(D) highlight different layers. Lines are guides to the eye, and arrows refer to the orthorhombic (top) and hexagonal (bottom) axes.

gated layers separated from the Yb-layers. The shortest H-H distance (d_{HH}) inside a layer is 2.64 Å. The high-P transition renders a relatively irregular arrangement into a highly symmetric crystal, by transferring half of all H(D) into planar interstitials of the Yb-layers. By this mechanism, the in-plane d_{HH} becomes larger and equal to 3.56 Å, whereas the shortest d_{HH} between neighboring planes reduces only slightly to 2.37 Å. This picture is confirmed by phonon calculations in the high-P phase, where its low-pressure instability is driven by a phonon softening at $\mathbf{q} = \mathbf{M}$. The related distortion implies the doubling of the hexagonal unit cell, with a phonon pattern that brings this structure back to the known α -phase [20].

Such an H arrangement seems to be unique among all hexagonal transition and rare earth (RE) hydrides where the hydrogen positions are known from by neutron diffraction. In the well-studied monohydrides FeH and CrH hydrogen is located exclusively at the octahedral sites between the hcp layers [21, 22]. In the hexagonal rare-earth hydrides (all with compositions REH_3) it is located at both octahedral and tetrahedral sites, or close

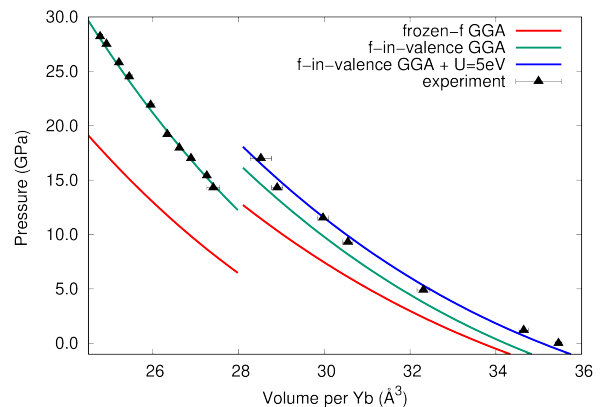


FIG. 4. EOS for α - and high-P phases by *ab initio* calculations with different flavors, and compared with experiment for YbH_2 [11]. DFT-GGA calculations with the PBE functional are shown in red and green, for the frozen- f and f -in-valence PAW pseudopotentials, respectively. DFT-GGA calculations with f -in-valence pseudopotential plus Hubbard repulsion (GGA+U) are shown in blue for the α -phase.

to them, i.e. again *between* the metal planes [23]. High-P YbH_2 seems therefore to be the only hydride known up to now adopting a structure of this type.

Knowing the structure of YbD_2 allows us to derive electronic properties through first-principles calculations at fixed experimental geometries. We carried out density functional theory (DFT) calculations within the generalized gradient approximation (GGA) built in the PBE functional [24, 25]. We used the plane-waves implementation as coded in the QUANTUM ESPRESSO package [26] [27]. The key question we address here is about the f -electrons role in driving the structural transition. Hypotheses have been made about a possible valence change in YbH_2 between the α - and high-P phase, where a tight competition between the atomic $4f^{14}(5d6s6p)^2$ ($2+$) and $4f^{13}(5d6s6p)^3$ ($3+$) configurations could be at play [11]. Yb and Eu are the rare-earth element where divalent and trivalent states are the closest in energy [28], and they are the only ones where the $2+$ valence is the most stable in the solid state at ambient pressure [29]. To investigate the role of the f electrons in YbH_2 , we ran two types of calculations. One with the f manifold frozen in the Yb pseudopotential, the other with in-valence f electrons. Both pseudopotentials (PAW type) are fully relativistic and keep the $5s5p$ semicore states in valence [30].

The results for the EOS are shown in Fig. 4 and compared with experimental data for YbH_2 [11]. The geometries used in our DFT calculations have both Yb and H positions determined from experiment [31]. The frozen- f calculations poorly reproduce the experimental EOS, with a significant pressure discrepancy at the phase transition. The f -in-valence calculations substan-

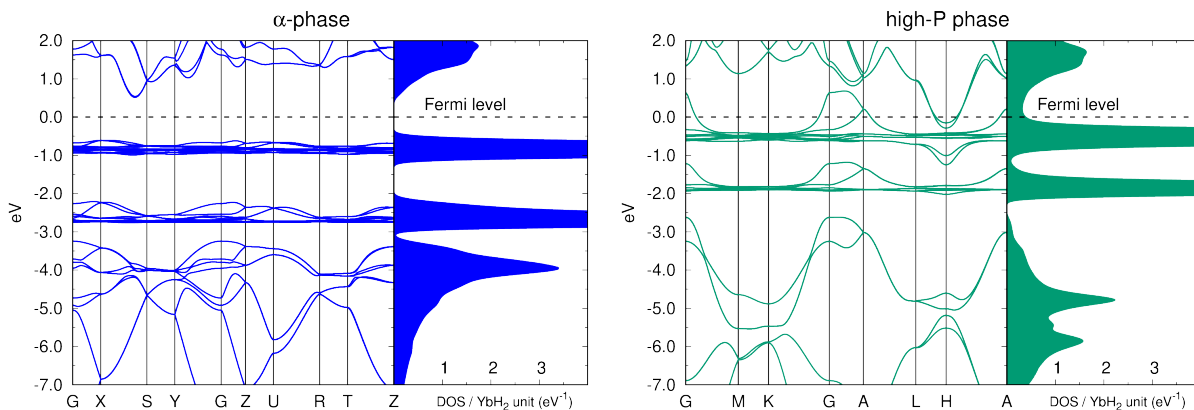


FIG. 5. Band structure and DOS for the α -phase at ambient pressure (left panel), and for the high-P phase at 26 GPa (right panel). In both cases, calculations are done with the fully relativistic PBE functional and f -in-valence PAW pseudopotentials.

tially improve the agreement with the experiment, signaling the importance of the structural feedback on the f -bands shape. In the α -phase, the agreement is further improved by including an Hubbard repulsion term within the DFT+U scheme [32], while in the high-P phase the agreement between theory and experiment is very good already at the DFT level. This points towards an f -manifold more correlated in the α - than in the high-P phase. The experimental knowledge of both Yb and H positions gives us a unique chance to assess the validity of the GGA approximation with f -in-valence electrons for this kind of systems. Other widely used DFT approximations, such as the local density one (LDA), turn out to perform more poorly, as shown by additional calculations we report as Suppl. Material (SM) [20].

To gain insight into the role played by the f electrons as valence states we plot in Fig. 5 the band structure and the density of states (DOS) at ambient and high pressure for the approximations reproducing best the experimental EOS, i.e. the DFT and DFT+U for the high-P and α -phase, respectively. The ambient-pressure phase is a semiconductor, in agreement with experiment, with a gap of about 1 eV between the empty states (mainly of d character) and the narrow $f_{j=7/2}$ bands. In contrast, the f manifold in the high-P phase has a much wider bandwidth, because of strong hybridization with the d states. This is a typical signature of the f -electrons delocalization. The f states are pushed up in energy, and the $f_{7/2}$ multiplet crosses the Fermi level. The high-P phase is hence clearly a metal. The $f_{j=7/2}$ - $f_{j=5/2}$ splitting of more than 1 eV is a straightforward manifestation of the strong spin-orbit coupling (SOC) in YbH_2 . While this splitting significantly reduces the bandgap in the insulating α -phase, the fermiology of the metallic phase seems to be only marginally affected by SOC (see SM [20]).

The f -character change across the transition is also reflected by the atomic orbital occupation analysis, reported in Tab. I. One can see that the $P6_3/mmc$ -phase is

in a mixed valence configuration, through the formation of conducting $f_{7/2}$ -holes with fractional occupation (0.25 per YbH_2 unit at 26 GPa). There is also a simultaneous increase of the $5d$ occupation and a slight depletion of the $6s6p$ manifold. In other words, the structural transition is accompanied by a charge transfer towards the d orbitals, and by the partial delocalization of f holes. Both phenomena are responsible for a tighter chemical bond between two neighboring Yb atoms, whose distance is indeed much shorter in the high-P phase [33].

TABLE I. Atomic orbital occupations per YbH_2 unit for the α - (ambient pressure) and high-P (26 GPa) phases.

Orbital symmetry	α	high-P
$4f(\text{Yb})$	14.00	13.75
$5d(\text{Yb})$	1.30	1.80
$6s6p(\text{Yb}) + 1s(\text{H}_2)$	2.70	2.45

The hybridization between the $4f$ and $5d$ orbitals increases the f bandwidth and thereby reduces correlations. This rationalizes the fact that the EOS of the high-P phase is well described already at the DFT level, while in the α -phase, showing very flat f -electrons and band-insulating character, the addition of an explicit Hubbard term seems necessary for a quantitative agreement with the experiment. It is interesting to note that, qualitatively, one can get the same physical picture for the transition even without U. The only difference is a smaller bandgap in the α phase (0.2 eV) and, consequently, a lower transition pressure obtained by standard GGA (see Fig. 4 and SM [20]). We verified that the metallicity of this phase is robust against the possible occurrence of magnetic order arising from the f -hole moments [34]. Neither a ferromagnetic nor an inter-layer antiferromagnetic order is a stable ground state at the DFT level.

Given its metallic character, superconductivity in high-P YbH_2 appears a possibility to explore. Calculations

reveal a non-negligible electron-phonon coupling involving the out-of-plane modes of interstitial hydrogen at 26 GPa. However, the total integrated coupling is not large enough to yield a sizable T_c at these pressures [20]. Superconductivity could nevertheless emerge at higher pressures, possibly driven by enhanced charge fluctuations [35] in the mixed-valence regime.

This work is based on experiments performed at the Japanese neutron spallation source MLF under proposal number 2018A0276. DFT calculations benefited from computer resources made available by the GENCI allocation under the project number A0030906493, and by the PRACE project under proposal number 2016163936. S.K. acknowledges financial support through a joint CNRS-JSPS travel grant No. PRC2191.

* Corresponding author: Stefan.Klotz@upmc.fr

- [1] A. Drozdov, I. Erements, I. Troyan, V. Ksenofontov, and S. Shylin, *Nature* **525**, 73 (2015).
- [2] D. Duan, Y. Liu, Y. Ma, Z. Shao, B. Liu, and T. Ciu, *Nat. Sci. Review* **4**, 121 (2016).
- [3] M. Somayazulu, M. Ahart, A. Mishra, Z. Geballe, M. Badini, Y. Meng, V. Struzhkin, and R. Hemley, *Phys. Rev. Lett.* **122**, 027001 (2019).
- [4] F. Peng, Y. Sun, C. Pickard, R. Needs, Q. Wu, and Y. Ma, *Phys. Rev. Lett.* **119**, 107001 (2017).
- [5] J. Song, G. Fabbris, W. Bi, D. Haskel, and J. S. Schilling, *Phys. Rev. Lett.* **121**, 037004 (2018).
- [6] E. Bucher, P. Schmidt, A. Jayaraman, K. Andres, J. Maita, K. Nassau, and P. Dernier, *Phys. Rev. B* **2**, 3911 (1970).
- [7] J. Lock, *Proc. of the Phys. Soc. Section B* **70**, 476 (1957).
- [8] K. Syassen, G. Wortmann, J. Feldhaus, K. H. Frank, and G. Kaindl, *Phys. Rev. B (Rapid)* **26**, 4745 (1982).
- [9] C. Dallera, O. Wesseley, M. Colarieti-Tosti, O. Eriksson, R. Ahuja, B. Johansson, M. Katsnelson, E. Annesse, J.-P. Rueff, G. Vanko, L. Braicovich, and M. Grioni, *Phys. Rev. B* **74**, 081101 (2006).
- [10] B. Lebeck, N. Hessel Andersen, S. Steenstrup, and A. Schroder Pedersen, *Acta Cryst.* **C39**, 1475 (1983).
- [11] J. Olsen, B. Buras, L. Gerward, B. Johansson, B. Lebeck, H. Skriver, and S. Steenstrup, *Physica Scripta* **29**, 503 (1984).
- [12] J. Olsen, S. Steenstrup, and L. Gerward, *Proc. XVth AIRAPT & XXXIII EHPRG Conf. Warsaw, Poland, W.A. Trzeciakowski (ed.)*, 549 (1996).
- [13] I. Goncharenko, M. Erements, M. Hanfland, J. Tse, M. Amboage, Y. Yao, and I. Trojan, *Phys. Rev. Lett.* **100**, 045504 (2008).
- [14] B. Li, Y. Ding, D. Y. Kim, R. Ahuja, G. Zou, and H.-K. Mao, *PNAS* **108**, 18618 (2001).
- [15] C. P. Pépin, A. Dewaele, G. Geneste, P. Loubeyre, and M. Mezouar, *Phys. Rev. Lett.* **113**, 265504 (2014).
- [16] T. Hattori, A. Sano-Furukawa, H. Arima, K. Komatsu, Y. Yamada, Y. Inamura, T. Nakatani, Y. Seto, T. Nagai, W. Utsumi, T. Itaka, H. Kagi, Y. Katayama, T. Inoue, T. Otomo, K. Suzuya, T. Kamiyama, M. Arai, and T. Yagi, *Nucl. Instrum. Meth. Phys. Res. A* **780**, 55 (2015).
- [17] S. Klotz, *Techniques in High Pressure Neutron Scattering*, Taylor and Francis, CRC, Boca Raton (2013).
- [18] T. Hattori, A. Sano-Furukawa, S. Machida, K. Funakoshi, H. Arima, and N. Okazaki, *High Press. Res.* **39**, 417 (2019).
- [19] J. Rodríguez-Carvajal, *Physica B* **192**, 55 (1993).
- [20] See Supplemental Material at [URL will be inserted by publisher] for the determination of the hydrogen/deuterium location through the simulation of the neutron diffraction pattern, the thermal expansion of RE dihydrides [36], the assesment of pseudopotentials, density functionals, Hubbard and SOC interactions by direct comparison with experimental geometries and EOS, the structural instability studied by means of phonon calculations, the el-ph coupling calculations. All files related to a published paper are stored as a single deposit and assigned a Supplemental Material URL. This URL appears in the article's reference list.
- [21] V. Antonov, M. Baier, B. Dorner, V. Fedotov, G. Grosse, A. Kolznikov, E. Ponyatovsky, G. Schneider, and F. Wagner, *J. Phys.: Condens. Matter* **14**, 6427 (2002).
- [22] G. Albrecht, F. Doenitz, K. Kleinstuck, and M. Betzl, *Phys. Stat. Solidi* **3**, K249 (1963).
- [23] K. Mackay, *Hydrogen Compounds of the Metallic Elements*, E.F.N. Spon Ltd, London (1966).
- [24] J. P. Perdew, K. Burke, and M. Ernzerhof, *Phys. Rev. Lett.* **77**, 3865 (1996).
- [25] J. P. Perdew, K. Burke, and M. Ernzerhof, *Phys. Rev. Lett.* **78**, 1396 (1997).
- [26] P. Giannozzi, S. Baroni, N. Bonini, M. Calandra, R. Car, C. Cavazzoni, D. Ceresoli, G. L. Chiarotti, M. Cococcioni, I. Dabo, A. D. Corso, S. de Gironcoli, S. Fabris, G. Fratesi, R. Gebauer, U. Gerstmann, C. Gougousis, A. Kokalj, M. Lazzeri, L. Martin-Samos, *et al.*, *J. Phys.: Condens. Matter* **21**, 395502 (2009); P. Giannozzi, O. Andreussi, T. Brumme, O. Bunau, M. B. Nardelli, M. Calandra, R. Car, C. Cavazzoni, D. Ceresoli, M. Cococcioni, N. Colonna, I. Carnimeo, A. D. Corso, S. de Gironcoli, P. Delugas, R. A. DiStasio, A. Ferretti, A. Floris, G. Fratesi, G. Fugallo, *et al.*, *ibid.* **29**, 465901 (2017).
- [27] The calculations used a plane-wave cutoff of 120 Ry for the wave function and 480 Ry for the charge, a $8 \times 8 \times 8$ electron \mathbf{k} -grid and a Methfessel-Paxton smearing of 0.01 Ry in the integration in a self-consistent loop. Further calculations with a $32 \times 32 \times 32$ grid and tetrahedra interpolation were performed for more accurate computations of the DOS and the Fermi level, starting from a previously converged $8 \times 8 \times 8$ self-consistent electron density.
- [28] B. Johansson, *Phys. Rev. B* **20**, 1315 (1979).
- [29] P. Strange, A. Svane, W. Temmerman, Z. Szotek, and H. Winter, *Nature* **399**, 756 (1999).
- [30] The pseudopotentials have been generated using the ATOMIC code of the QUANTUM ESPRESSO package [26]. The reference atomic calculation is done in the $[\text{Xe}]4f^{14.0}5d^{0.0}6s^{1.5}6p^{0.5}$ electronic configuration. Non-linear core corrections have been used.
- [31] The unit cell of the high-P structure has only two variables, i.e. a and c . The volume was varied by changing a , while keeping $c/a = 1.33$ fixed at its 26 GPa value. For the α -phase, a , b , and c and internal coordinates were determined by experiment at ambient pressure. We fixed the ambient-pressure values of $b/a = 0.606$, $c/a = 1.15$,

and the internal atomic positions, and changed a to vary the volume. The variation of b/a and c/a is marginal in the volume range spanned by our calculations.

- [32] We used the DFT+U formulation of Refs. 37 and 38 with $U = 5$ eV, $J = 0.5$ eV, and F_4/F_2 and F_6/F_2 Slater integral ratios taken from their atomic values. The U and J values are those of Ce [39], assuming an electron-hole symmetry in the f manifold. We verified that the same value of U is optimal to reproduce the EOS in Fig. 4.
- [33] At 22 GPa, the Yb-Yb out-of-plane distance in the high-P phase is 3.167 Å against an average of 3.34 Å in the α -phase, while for the in-plane Yb-Yb distance we find 3.37 Å in the high-P phase versus 3.435 Å (average) in the α -phase.
- [34] W. Iwasieczko, M. Drulis, and H. Drulis, *J. Alloys Compd.* **327**, 11 (2001).
- [35] E. R. Ylvisaker, J. Kuneš, A. K. McMahan, and W. E. Pickett, *Phys. Rev. Lett.* **102**, 246401 (2009).
- [36] J. Bonnet and J. Daou, *Journal of Applied Physics* **48**, 964 (1977).
- [37] V. Anisimov, J. Zaanen, and O. Andersen, *Phys. Rev. B* **44**, 943 (1991).
- [38] A. Liechtenstein, V. Anisimov, and J. Zaanen, *Phys. Rev. B* **52**, R5467 (1995).
- [39] F. Nilsson, R. Sakuma, and F. Aryasetiawan, *Phys. Rev. B* **88**, 125123 (2013).